Mathematics

http://www.aimspress.com/journal/Math

AIMS Mathematics, 8(1): 1427–1454.
DOI: 10.3934/math.2023072
Received: 10 May 2022
Revised: 31 August 2022
Accepted: 06 September 2022
Published: 20 October 2022

Research article

An efficient hybridization scheme for time-fractional Cauchy equations with convergence analysis

Saud Fahad Aldosary[1,*], Ram Swroop[2], Jagdev Singh[3], Ateq Alsaadi[4] and Kottakkaran Sooppy Nisar[1]

[1] Department of Mathematics, College of Arts and Sciences, Wadi Aldawaser, Prince Sattam bin Abdulaziz University, Saudi Arabia

[2] Department of Mathematics, Arya College of Engineering and IT, Kukas, Jaipur, Rajasthan 302028 India

[3] Department of Mathematics, JECRC University, Jaipur-303905, Rajasthan, India

[4] Department of Mathematics and Statistics, College of Science, Taif University, P.O. Box 11099, Taif 21944, Saudi Arabia

* **Correspondence:** Email: sau.aldosary@psau.edu.sa.

Abstract: In this paper, a time-fractional Cauchy equation (TFCE) is analyzed by using the q-homotopy analysis Shehu transform algorithm (q-HASTA) with convergence analysis. The q-HASTA comprises with the reduced differential transform algorithm (RDTA). The solution of TFCE is represented in the series form by using the q-HASTA scheme. The TFCE is transformed into algebraic form for finding the general solution efficiently. This provides a compact form solution with minimized error. There are three key outcomes of the work. First, the small size of input parameters by the RDTA transforms into the subsidiary equation so that it takes short time to solve. As the second advantage, the structure of the problem is reduced by controlling the solution series; hence the characterization of the solution becomes classified for finding the particular solution. The third advantage of this work is that the approximate solution with absolute error approximation for the fractional model of the problem is handled by using a generalized and efficient scheme q-HASTA. These outcomes are illustrated by graphs and tables.

Keywords: time-fractional Cauchy equation; q-homotopy analysis Shehu transform algorithm; reduced differential transform algorithm; Shehu transform
Mathematics Subject Classification (2010): 34A08, 35A20, 35A22, 35C05

1. Introduction

The fractional calculus, and its application, have proved itself as an optimal method to study the real world problems. This branch of applied analysis has been used in various domains of science, engineering and technology [1–7]. In 2013, Bulut et al. [8] analyzed the time-fractional generalized Burger equation and trial equations for optimizing the wave equation. He [9] presented the compact solution in porous media for seepage flow equation in 1998. In 2020, Dubey et al. [10] examined the fractional order computer virus propagation model. Kumar et al. [11] presented the mathematical model for chemical system. Singh et al. [12] examined the fractional order multi-dimensional diffusion problems.

In 2015, Ramswaroop et al. [13] presented the new computational method for a biological system as fractional Lotka-Volterra application. Ghanbari and Kumar [14] studied a fractional order predator-prey model with Beddington-DeAngelis functional response by using a numerical scheme. Zhou [15] gave variation iteration method for solving Cauchy equation. A detailed analysis of Cauchy problems have been given in several works [16–18]. Dubey et al. [19] studied fractional order Black-Scholes European option pricing model. Recently, Maitama et al. [20,21] proposed an integrated fractional transformation for analyzing the steady heat transfer problem. In 2019, the Caputo-fractional differential equation is analyzed by an improved Shehu transformation by Belgacem et al. [22]. Bokhari et al. [23] presented a novel application of the Shehu transformation for solving Atangana-Baleanu derivatives in 2019. El-Tawil [24,25] introduced the q-homotopy analysis method whose mechanism is based on homotopy which is generalized of the homotopy analysis method introduced and applied by Liao [26–29]. In 2018, Noeiaghdam et al. [30] applied homotopy analysis on a modified epidemiological model of computer viruses. In 2021, Noeiaghdam et al. [31] approached homotopy analysis transform method for the nonlinear bio-mathematical model of malaria infection. In 2021, Noeiaghdam et al. [32] presented a nonlinear fractional order model of COVID-19. In 2016, Noeiaghdam et al. [33] applied homotopy analysis transform for solving Abel's integral equations of first kind. In 2017, Singh et al. [34] introduced an efficient method for solving the time fractional Rosenau-Hyman equation. In 2010, Keskin et al. [35] introduced a new method based on fractional PDE. This method is applied for reducing the domain of differential transformation. Gupta [36] analyzed fractional Bennery-Lin equation by fractional PDE in 2011. The key outcome of this approach is, the discreteness of approximate solutions. Srivastava et al. [37] defined the RDTM solutions over the Caputo-time fractional order hyperbolic telegraph equation. In recent years several methods and applied aspects for fractional calculus have been studied by many authors [38–42].

In this paper, the time-fractional Cauchy problem is analyzed by the q-HASTA and the RDTA over the Caputo's sense fractional derivatives. The q-HASTA is a well coupling of the q-HAM. The homotopical approach comprises with differential topology, the Shehu transform and the Laplace-type integral transform [20–23]. The q-HAM [24,25] is an extension of homotopy analysis methods [26–30]. The RDTA technique is an optimized method developed by Keskin et al. [35]. There are 3 key outcomes of this paper stated as, small parameters, compact system of equation and approximate functional range. Thus, the proposed method is referred as the efficient and compact with respect to time and computations. The initial equation is introduced next.

The time fractional Cauchy differential equation as follows:

$$D_\tau^\eta w(\zeta,\tau) + \delta(\zeta,\tau) w_\zeta(\zeta,\tau) = \beta(\zeta), \;\; 0 < \eta \;\leq 1, \;\; \tau > 0, \tag{1.1}$$

$$w(\zeta,0) = \psi(\zeta), \;\; \zeta \in R. \tag{1.2}$$

If $\delta(\zeta,\tau) = \delta(\text{constant})$, $\beta(\zeta) = 0$ and $\eta = 1$, Eq (1.1) is called as the transport equation [16,18] that can play crucial role in the moving of wind and the spread of AIDS. If we assume $\delta(\zeta,\tau) = w(\zeta,\tau)$, $\eta = 1$ the Eq (1.2) is formed as the inviscid Burgers' equation [17,18] approaches the one-dimensional stream of particles have zero viscosity. Next, the pre-requisites are given.

2. Preliminaries

This section presents the applied notations, feature and definitions related to fractional calculus deals with generalization of integer order derivatives and integrations.

Definition 2.1. [43] A real function $£(\tau), \tau > 0$ is said to be in the space $C_\upsilon, \upsilon \in R$ if there exists a real number$\rho(> \upsilon)$, such that $£(\tau) = \tau^\rho \beta(\tau)$, where $\beta(\tau) \in C\,[0,\infty)$, and its said to be in the space C_υ^n if and only if $£^{(\mathrm{n})} \in C_\upsilon; n \in N$.

Definition 2.2. If $n \in N, n-1 < \eta \leq n$, the derivative property of the Laplace transform in the Caputo sense $D_\tau^\eta £(\tau)$ is obtained by the Caputo [1,2] and Kilbas et al. [3] in the form

$$L\{D_\tau^\eta £(\tau)\} = s^\eta L\{£(\tau)\} - \sum_{k=0}^{n-1} s^{\eta-k-1} £^{(k)}(0^+). \tag{2.1}$$

Definition 2.3. For $\eta > 0, £(\tau) \in C_\nu, \nu \geq -1$, the Riemann-Liouville fractional integral $\mathrm{I}^\eta £(\tau)$ is expressed as

$$I^\eta £(\tau) = \begin{cases} \frac{1}{\Gamma(\eta)} \int_0^\tau (\tau - t)^{\eta-1} £(\tau) d\tau, & \eta > 0, \; \tau > 0, \\ £(\tau), & \eta = 0. \end{cases} \tag{2.2}$$

Definition 2.4. For $n \in N, n-1 < \eta \leq n$, $£(\tau) \in C_\nu^n, \nu \geq -1, \tau > 0$, then the Caputo [1] fractional derivative of $£(\tau)$ is illustrated as

$$D_\tau^\eta £(\tau) = \frac{1}{\Gamma(n-\eta)} \int_0^\tau (\tau - t)^{n-\eta-1} £^n(\tau) dt. \tag{2.3}$$

Definition 2.5. The fractional derivative property of Shehu transform in the Riemann-Liouville form, [20] if $n-1 < \eta \leq n, \eta > 0$,$r = 1 + [\eta]$and $£(\tau), I^{r-\eta}£(\tau), \frac{d}{d\tau} I^{r-\eta}£(\tau), \cdots, \frac{d^r}{d\tau^r} I^{r-\eta}£(\tau), D_\tau^\eta £(\tau) \in A$, was obtained by

$$S\,[D^\eta £(\tau)] = (\frac{s}{u})^\eta S\,[£(\tau)] - \sum_{k=0}^{r-1} \left(\frac{s}{u}\right)^{r-k-1} \frac{d^{k-1}}{d\tau^{k-1}} I^{r-\eta} £(0^+). \tag{2.4}$$

And the Caputo form, [21] if $\eta > 0$, $r = 1 + [\eta]$and $£(\tau), \frac{d}{dt}£(\tau), \cdots, \frac{d^r}{dt^r}£(\tau), D^\eta £(t) \in A$, was obtained by the Caputo [1,2] as

$$S\,[D_\tau^\eta £(\tau)] = (\frac{s}{u})^\eta S\,[£(\tau)] - \sum_{k=0}^{r-1} \left(\frac{s}{u}\right)^{r-k-1} \frac{d^{k-1}}{d\tau^{k-1}} £^{(\mathrm{k})}(0^+). \tag{2.5}$$

Definition 2.6. Let we consider $V(s,u)$ denote the Shehu transform of $v(\tau)$, and then the inverse Shehu transform is given by [21]; defined as

$$v(\tau) = S^{-1}\left[V(s,u)\right] = \lim_{p\to\infty}\frac{1}{2\pi i}\int_{\eta-i\rho}^{\eta+i\rho}\frac{1}{u}\exp\left(\frac{s\tau}{u}\right)V(s,u)ds,\, s>0,\ \ u>0. \tag{2.6}$$

3. Analysis of q-HASTA

We analysis the q-HASTA for a general fractional differential equation of order η given in the following manners:

$$D_\tau^\eta w(\zeta,\tau) + R\,w(\zeta,\tau) + N w(\zeta,\tau) = \kappa(\zeta,\tau),\ \ \tau>0,\, n-1<\eta\le n, n\in N. \tag{3.1}$$

Where $D_\tau^\eta w(\zeta,\tau)$ denote the fractional Caputo derivative of $w(\zeta,\tau)$, R and N are the linear and the nonlinear differential operators respectively, $\kappa(\zeta,\tau)$ denoted the source term.

Next, we employ the Shehu transform on Eq (3.1), we get

$$S\left[D_\tau^\eta w\right] + S\,\left[Rw\right] + S\left[N\,w\right] = S\,\left[\kappa(\zeta,\tau)\right]. \tag{3.2}$$

Using the result of Shehu transform for Caputo fractional derivative, we get

$$S\left[w\right] - \left(\frac{u}{s}\right)^\eta\sum_{k=0}^{n-1}s^{\eta-k-1}w^{(k)}(\zeta,0) + \left(\frac{u}{s}\right)^\eta\left[S\left[Rw\right] + S\left[N\,w\right] - S\left[\kappa(\zeta,\tau)\right]\right] = 0. \tag{3.3}$$

We involved the nonlinear operator as

$$\begin{aligned}\mathrm{N}[\chi(\zeta,\tau\,;\rho)] = S\left[\chi(\zeta,\tau\,;\rho)\right] - \left(\tfrac{u}{s}\right)^\eta\textstyle\sum_{k=0}^{n-1}s^{\eta-k-1}\chi^{(k)}(\zeta,\tau\,;\rho)(0^+)\\ +\left(\tfrac{u}{s}\right)^\eta\left[S\left[R\chi(\zeta,\tau\,;\rho)\right] + S\left[N\chi(\zeta,\tau\,;\rho)\right] - S\left[\kappa(\zeta,\tau)\right]\right] = 0.\end{aligned} \tag{3.4}$$

Now we use the classical HAM and a homotopy equation is presented as

$$(1-n\rho)\,S\,\left[\chi(\zeta,\ \tau\,;\rho) - w_0(\zeta,\tau)\right] = \hbar\,\rho H(\zeta,\tau)\,N\left[w(\zeta,\tau\,)\right], \tag{3.5}$$

where S is the Shehu transform operator, $\rho\in[0,\,\frac{1}{n}], n\ge 1$ and $\hbar\ne 0$ are the embedding parameter and auxiliary parameter respectively, $H(\zeta,\tau)$ a non-zero auxiliary function, $w_0(\zeta,\tau)$ is an basis assumption of $w(\zeta,\tau)$ and $\chi(\zeta,\tau\,;\rho)$ is a unknown real function which construct the following result

$$\chi(\zeta,\tau\,;\rho) = \begin{cases} w_0(\zeta,\tau), & \rho = 0,\\ w\ (\zeta,\tau), & \rho = \frac{1}{n}.\end{cases} \tag{3.6}$$

Consequently, as ρ goes from 0 to $\frac{1}{n}$, the solution $\chi(\zeta,\ \tau\,;\ \rho)$ converge from the initial guess $w_0(\zeta,\tau)$ to the solution $w(\zeta,\tau)$. Expressing of $\chi(\zeta,\tau\,;\ \rho)$ as the Taylor's series form with respect to ρ, as

$$\chi(\zeta,\tau\,;\rho) = w_0(\zeta,\tau) + \sum_{m=1}^{+\infty}w_m(\zeta,\tau)\,\rho^m, \tag{3.7}$$

where

$$w_m(\zeta,\ \tau) = \frac{1}{m\,!}\frac{\partial^m \chi(\zeta,\ \tau;\ \rho)}{\partial \rho^m}\Big|_{\rho=0}. \tag{3.8}$$

If we select appropriate values of the initial guess, auxiliary linear operator, the auxiliary parameter and the auxiliary function, the series (3.7) converges at $\rho = \frac{1}{n}$, then it provides the solutions of the given problem Eq (3.1), in the form

$$w(\zeta,\ \tau) = w_0(\zeta,\ \tau) + \sum_{m=1}^{+\infty} w_m(\zeta,\ \tau)(\frac{1}{n})^m. \tag{3.9}$$

And the governing equation can be deduced from the zero deformation Eq (3.5).

Now differentiate the zero-order deformation Eq (3.5) m-times with respect to ρ and taking $\rho = 0$ and finally dividing them by $m\,!$, it yields

$$S\,[w_m(\zeta,\ \tau) - k_m w_{m-1}(\zeta,\ \tau)] = \hbar\, H(\zeta,\ \tau)\mathfrak{R}_m(\vec{w}_{m-1}). \tag{3.10}$$

We define the vectors as

$$\vec{w}_m = \{w_0(\zeta,\,\tau),\ \ w_1(\zeta,\,\tau),\ \ w_2(\zeta,\tau), \ldots,\ \ w_m(\zeta,\,\tau)\}. \tag{3.11}$$

Taking the inverse Shehu transform on Eq (3.10), we have

$$w_m(\zeta,\,\tau) = k_m w_{m-1}(\zeta,\ \tau) + \hbar\, S^{-1}[H(\zeta,\ \tau)\mathfrak{R}_m(\vec{w}_{m-1})], \tag{3.12}$$

where $\mathfrak{R}_m(\vec{w}_{m-1})$ is given as

$$\mathfrak{R}_m(\vec{w}_{m-1}) = \frac{1}{(m-1)!}\left[\frac{\partial^{m-1} N\,[\chi(\zeta,\ \tau\,;\rho)]}{\partial \rho^{m-1}}\right]\Bigg|_{\rho=0}, \tag{3.13}$$

and

$$k_m = \begin{cases} 0 & if\ m\ \le\ 1, \\ n & if\ m\ >\ 1. \end{cases} \tag{3.14}$$

Finally, we solve the Eq (3.12) and we compute $w_m(\zeta,\tau)$ for $m \ge 1$, selecting appropriate parameter $\hbar$ and n, we deduce the q-HASTA convergence solution series as

$$w(\zeta,\tau) = w_0(\zeta,\tau) + \sum_{m=1}^{+\infty} w_m(\zeta,\tau)(\frac{1}{n})^m. \tag{3.15}$$

Theorem 3.1. If appropriate selection of convergences control parameters $\hbar \neq 0, n \geq 1$,and also suitable selection of $H(\zeta,\tau) \neq 0, w_0(\zeta,\tau)$, in Eq (3.12) such that $\|w_{m+1}\| \le \left(\frac{\Phi}{n}\right)\|w_m\|$, $0 < \Phi < n$, then the solution series $\sum_{m=0}^{+\infty} w_m(\zeta,\tau)(1/n)^m$,uniformly convergence, where $\|\cdot\|_\infty$ presented the appropriate norm.

Proof. We prove that the sequence $\langle\vartheta_m\rangle_{m=0}^{\infty}$, is the Cauchy sequence. Let's assume that ϑ_m,is the sequence of partially sums of $\vartheta_m = \sum_{k=0}^{m} w_k(\zeta,\tau)(1/n)^k$.

By observation, we have

$$\|\vartheta_{m+1} - \vartheta_m\| = \|w_{m+1}\| \le (\Phi/n)\|w_m\| \le (\Phi/n)^2\|w_{m-1}\| \le \cdots \le (\Phi/n)^{m+1}\|w_0\|.$$

For $\forall\, m \geq l,\ m, l \in N$, we deduced from the above equation

$$\begin{aligned}
\|\vartheta_m - \vartheta_l\| &= \|\vartheta_m - \vartheta_{m-1} + \vartheta_{m-1} - \vartheta_{m-2} + \vartheta_{m-2} - \vartheta_{m-3} + \cdots + \vartheta_{l+1} - \vartheta_l\| \\
&\leq \|\vartheta_m - \vartheta_{m-1}\| + \|\vartheta_{m-1} - \vartheta_{m-2}\| + \|\vartheta_{m-2} - \vartheta_{m-3}\| + \cdots + \|\vartheta_{l+1} - \vartheta_l\| \\
&\leq (\Phi/n)^m \|w_0\| + (\Phi/n)^{m-1} \|w_0\| + (\Phi/n)^{m-2} \|w_0\| + \cdots + (\Phi/n)^{l+1} \|w_0\| \\
&= \left((\Phi/n)^m + (\Phi/n)^{m-1} + (\Phi/n)^{m-2} + \cdots + (\Phi/n)^{l+1}\right) \|w_0\|, \\
&= \frac{\Phi^{m+1}}{n^m(n-\Phi)} \|w_0\|.
\end{aligned}$$

For $m, l \to \infty$, and then $\|\vartheta_m - \vartheta_l\| \to 0$. Therefore, the sequence $\langle \vartheta_m \rangle_{m=0}^{\infty}$, is a Cauchy sequence, hence convergence.

Table 1 gives the basic results of the Sehu transform.

Table 1. The basic results of the Shehu transform $S\,[w\,(\tau)] = \int_0^\infty \exp\left(\frac{-s\tau}{u}\right) w(\tau)\, d\tau\,;\ \ s > 0, u > 0.$

Original functions $w(\tau)$	The Shehu transformed function $S\,[w(\tau)] = W(s,u)$
1	u/s
$\tau^n;\ n = 0, 1, 2, 3, \cdots.$	$(u/s)^{n+1}$
$\exp(\beta(\tau))$	$u/s - \beta u$
$\cos(\tau)$	$us/s^2 + u^2$
$\sin(\tau)$	$u^2/s^2 + u^2$

4. Basic idea of the reduced differential transforms algorithm (RDTA)

To demonstrate the basis analysis of the RDTA, we take a function $j(\zeta, \tau)$ such as $j(\zeta, \tau) = \varepsilon(\alpha)\, \nu(\beta)$. According to the one dimension differential transform, we can be defined $j(\zeta, \tau)$ such as:

$$j\,(\zeta,\ \tau) = \sum_{\alpha=0}^{+\infty} \varepsilon(\alpha)\, \zeta^\alpha \sum_{\beta=0}^{+\infty} \nu(\beta)\, \tau^\beta = \sum_{\alpha=0}^{+\infty} \sum_{\beta=0}^{+\infty} J(\alpha, \beta)\, \zeta^\alpha \tau^\beta, \tag{4.1}$$

where $J(\alpha,\beta) = \varepsilon(\alpha)\, \nu(\beta)$ represent the spectrum of $j(\zeta, \tau)$.

The basis preliminaries and operations of the RDTA are defined below.

Definition 4.1. If $j(\zeta, \tau)$ is analytical and differentiable about the ζ and time scale τ in the interest domain, then the spectrum function [36,37]

$$R_D[j(\zeta, \tau)] = \frac{1}{\Gamma(k\eta + 1)} \left[\frac{\partial^\mu}{\partial \tau^\mu} j(\zeta, \tau)\right]_{\tau=\tau_0} \approx J_\mu(\zeta). \tag{4.2}$$

Which presented the fractional reduced transformed of $j(\zeta, \tau)$ and its inverse transform of $J_\mu(\zeta)$ defined as

$$R_D^{-1}[J_\mu(\zeta)] = \sum_{\mu=0}^{+\infty} J_\mu(\zeta)\, (\tau - \tau_0)^{\mu\eta} \approx j\,(\zeta, \tau), \tag{4.3}$$

where R_D is the reduced differential transform operator and it's inverse operator denoted by R_D^{-1}, [35].

From Eqs (4.2) and (4.3), we can see that

$$j(\zeta,\tau)=\sum_{\mu=0}^{+\infty}\frac{1}{\Gamma(\mu\eta+1)}\left[\frac{\partial^{\mu}}{\partial\tau^{\mu}}j(\zeta,\tau)\right]\Bigg|_{\tau=\tau_0}(\tau-\tau_0)^{\mu\eta}, \tag{4.4}$$

if we set $\tau=0$,in above Eq (4.4), it convert to

$$j(\zeta,\tau)=\sum_{\mu=0}^{+\infty}\frac{1}{\Gamma(\mu\eta+1)}\left[\frac{\partial^{\mu}}{\partial\tau^{\mu}}j(\zeta,\tau)\right]\Bigg|_{\tau=\tau_0}(\tau)^{\mu\eta}. \tag{4.5}$$

From the above, we noted that the reduced differential transform solution can be deduced by expansion of the power series.

Definition 4.2. If $w(\zeta,\tau)=R_D^{-1}[W_\mu(\zeta)], p(\zeta,\tau)=R_D^{-1}[P_\mu(\zeta)]$, and $*$ denote the convolution, indicate form of the multiplication of the RDTA in fractional form. The mathematical fractional operation of the RDTA is shown in the Table 2.

Table 2. The fundamental concepts of the RDTA.

Functions $j(\zeta,\tau)$	Reduced differential transformed function $R_D[j(\zeta,\tau)=J_\mu(\zeta)$
$w(\zeta,\tau)*p(\zeta,\tau)$	$W_\mu(\zeta)*P_\mu(\zeta)=\sum_{\ell=0}^{\mu}W_\ell(\zeta)*P_{\mu-\ell}(\zeta)$
$c_1w(\zeta,\tau)\pm c_2p(\zeta,\tau)$	$c_1W_\mu(\zeta)\pm c_2P_\mu(\zeta)$
$\left(\partial^{\aleph\eta}/\partial\tau^{\aleph\eta}\right)w(x,\tau)$	$(\Gamma(\mu\eta+\aleph\eta+1)/\Gamma(\mu\eta+1))\,W_{\mu+\aleph}(\zeta)$
$w(\zeta,\tau)p(\zeta,\tau)$	$\sum_{i=0}^{\mu}W_i(\zeta)P_{\mu-i}(\zeta)=\sum_{\ell=0}^{\mu}P_\ell(\zeta)W_{\mu-\ell}(\zeta)$
$\zeta^r\tau^n w(\zeta,\tau)$	$\zeta^r W_{\mu-n}(\zeta)$
$\zeta^r\tau^n$	$\zeta^r\delta(\mu-n)$
$e^{\lambda\tau}$	$\lambda^\mu/\Gamma(\mu+1)$

5. Numerical examples

Here we analysis the validities of both the proposed algorithm by series solution and graphical representations, taking auxiliary function$H(\zeta,\tau)=1$. We use $w=w(\zeta,\tau)$is the function of space coordinate $\zeta(\zeta\in R)$and time scale $\tau\,(\tau>0)$, a is arbitrary constant.

Example 1. We consider the following transpose equation [16–18] in fractional form

$$\frac{\partial^\eta w}{\partial\tau^\eta}+a\frac{\partial w}{\partial\zeta}=0, \tag{5.1}$$

and the initial conditions

$$w(\zeta,0)=w_0=\zeta^2. \tag{5.2}$$

Case 1: q-HASTA solution

Computing Shehu transform on Eq (5.1) with the initial condition (5.2) as

$$S\left[w(\zeta,\tau)\right]-\frac{u}{s}\zeta^2+\frac{u^\eta}{s^\eta}S\left[a\frac{\partial w(\zeta,\tau)}{\partial\zeta}\right]=0. \tag{5.3}$$

We presented the nonlinear operator as

$$\mathrm{N}\left[\chi(\zeta,\tau;\rho)\right] = S\left[\chi(\zeta,\tau;\rho)\right] - \frac{u}{s}\zeta^2 + a\frac{u^\eta}{s^\eta}S\left[\frac{\partial\chi(\zeta,\tau;\rho)}{\partial\zeta}\right], \tag{5.4}$$

and we have

$$\Re\left(\vec{w}_{m-1}\right) = S\left(\vec{w}_{m-1}\right) - \left(1-\frac{k_m}{n}\right)\frac{u}{s}\zeta^2 + a\frac{u^\eta}{s^\eta}\left[\frac{\partial\,\vec{w}_{m-1}}{\partial\zeta}\right]. \tag{5.5}$$

The mth-order deformed equation is defined as

$$S\left[w_m(\zeta,\tau) - k_m w_{m-1}(\zeta,\tau)\right] = \hbar\Re_m(\vec{w}_{m-1}). \tag{5.6}$$

By using the inverse Shehu transform of Eq (5.6)

$$w_m(\zeta,\tau) = k_m w_{m-1}(\zeta,\tau) + \hbar S^{-1}\left[\Re_m(\vec{w}_{m-1})\right]. \tag{5.7}$$

Simplifying the Eq (5.7), for $m = 1, 2, 3, \cdots$, and we get

$$\begin{aligned}
w_1(\zeta,\,\tau) &= 2a\,\zeta\,\hbar\frac{\tau^\eta}{\Gamma(\eta+1)},\\
w_2(\zeta,\tau) &= 2a\,\zeta\,\hbar\,(\hbar+n)\frac{\tau^\eta}{\Gamma(\eta+1)} + 2a^2\,\hbar^2\frac{\tau^{2\eta}}{\Gamma(2\eta+1)},\\
w_3(\zeta,\tau) &= 2a\,\zeta\,\hbar\,(\hbar+n)^2\frac{\tau^\eta}{\Gamma(\eta+1)} + 4a^2\,\hbar^2\,(h+n)\frac{\tau^{2\eta}}{\Gamma(2\eta+1)},\\
&\vdots
\end{aligned} \tag{5.8}$$

And so on, the components of $w_m(\zeta,\tau), m \geq 4$, can be easily obtained. The series solution is given as

$$w(\zeta,\tau) = w_0(\zeta,\tau) + \sum_{m=1}^{\infty} w_m(\zeta,\tau)\left(\frac{1}{n}\right)^m. \tag{5.9}$$

For $\hbar = -1$, $n = 1$ and $\eta = 1$ then clearly, the solution series (5.9) provides the solution and converges to the exact solution $w(\zeta,\tau) = \zeta^2 - 2a\zeta\tau + a^2\tau^2$, which is coincident to VIM [15].

Case 2: RDTA solution

We apply the RDTA to Eq (5.1), to obtain

$$\frac{\Gamma(m\eta+\eta+1)}{\Gamma(m\eta+1)}W_{m+1} = -a\frac{\partial W_m}{\partial\zeta}. \tag{5.10}$$

Applying the RDTA with initial condition (5.2), we have

$$\begin{aligned}
&W_0(\zeta) = \zeta^2,\\
&W_1(\zeta) = -2a\,\zeta\frac{1}{\Gamma(\eta+1)}, W_2(\zeta) = 2a^2\frac{1}{\Gamma(2\eta+1)}, W_3(\zeta) = 0,\\
&\vdots
\end{aligned} \tag{5.11}$$

and so on, in this way, we found the exact solution in second terms iteration, selecting $\eta = 1$. Using (5.11) we get the following approximations for the RDTA series solution

$$\begin{aligned} w(\zeta,\tau) &= \textstyle\sum_{m=0}^{3} W_m(\zeta)\,\tau^{m\eta} = W_0(\zeta) + W_1(\zeta)\,\tau^{\eta} + W_2(\zeta)\,\tau^{2\eta} + W_3(\zeta)\,\tau^{3\eta}. \\ &= \zeta^2 - 2a\zeta\frac{\tau^{\eta}}{\Gamma(\eta+1)} + 2a^2\frac{\tau^{2\eta}}{\Gamma(2\eta+1)}. \end{aligned} \tag{5.12}$$

Which is coincident obtained by the q-HASTA($\hbar = -1, n = 1$) and VIM [15] at $\eta = 1$, $\hbar = -1, n = 1$, given as

$$w(\zeta,\tau) = \zeta^2 - 2a\zeta\tau + a^2\tau^2. \tag{5.13}$$

The numerical analysis for the approximate series solution of Eq (5.1) obtained by using the q-HASTA & the RDTA with the exact solution (5.13) at $a = 0.01$ in Figures 1–5 are computed by using Maple package.

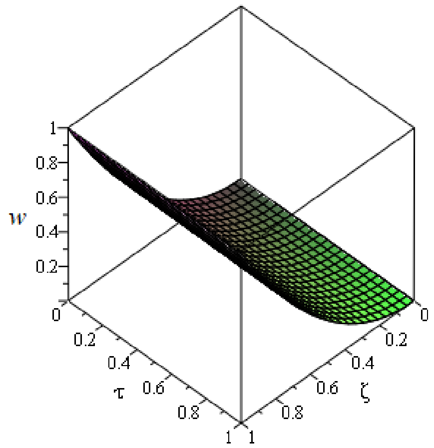

Figure 1. The surface shows the exact solution $w(\zeta,\tau)$ v/s space variable ζ and time variable τ.

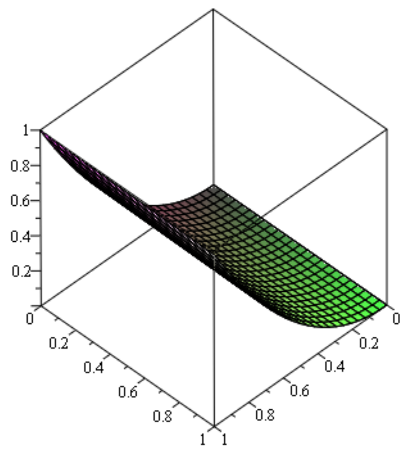

Figure 2. The surface shows the fractional order ($\eta = 0.9$), RDTA (q-HASTA, $\hbar = -1,\ n = 1$) solution $w(\zeta,\tau)$ v/s space variable ζ and time variable τ.

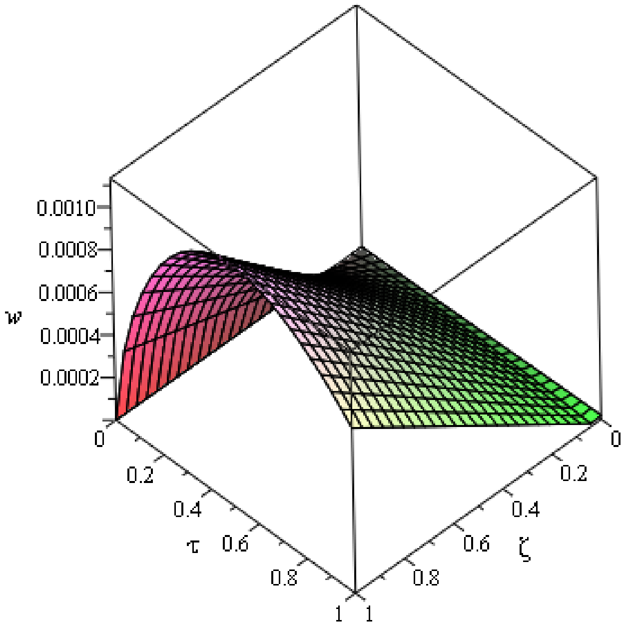

Figure 3. The surface represented the absolute error $E_3(w) = \left|w_{ex.} - w_{apr.}\right|$ v/s space variable ζ and time variable τ at $\hbar = -1, n = 1,\ \eta = 0.9$.

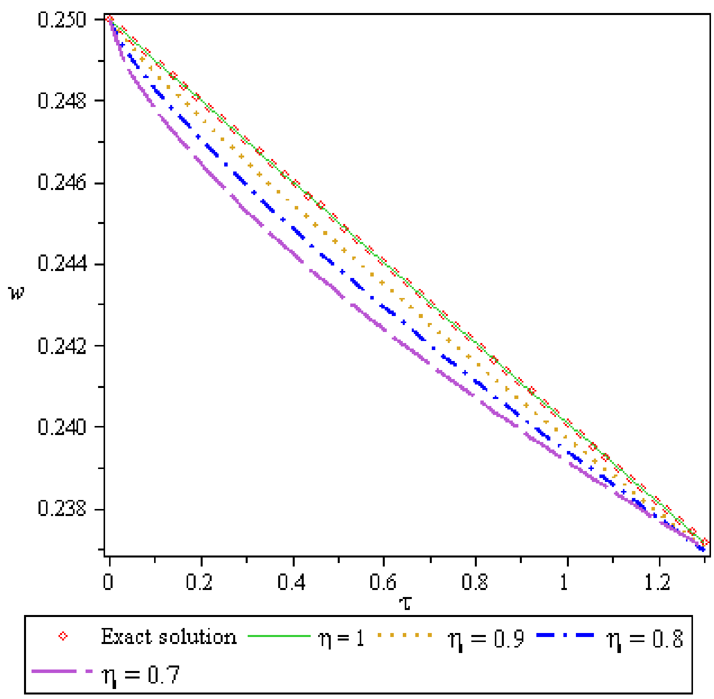

Figure 4. Response of family of RDTA (q-HASTA, $\hbar = -1,\ n = 1$) solution $w(\zeta, \tau)$ v/s time variable τ for varies values of η at space variable $\zeta = 0.5$.

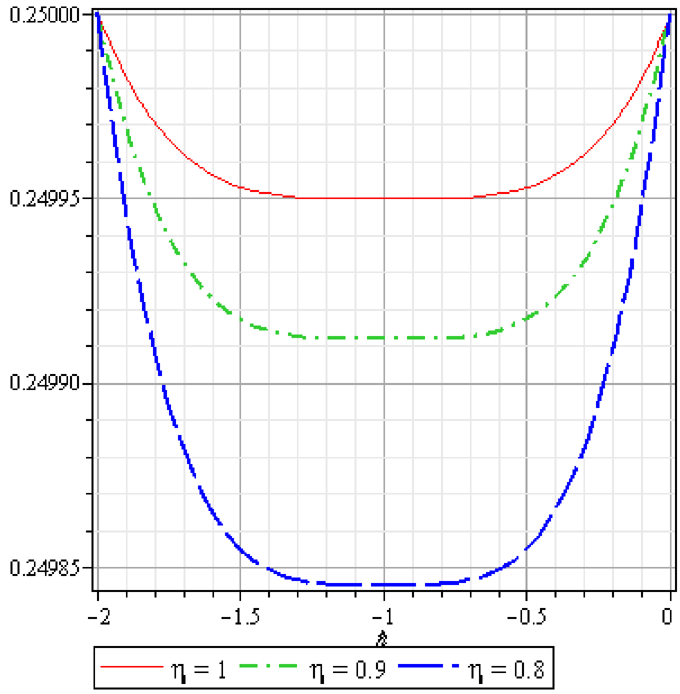

Figure 5. $\hbar - curves$ depicted comparative study of q-HASTA for varies η at $\zeta = 0.5$, $\tau = 0.005$ and $n = 1$.

Example 2. The fractional nonlinear equation with variable coefficients is given as

$$\frac{\partial^{\eta} w}{\partial \tau^{\eta}} + \zeta \frac{\partial w}{\partial \zeta} = 0, \tag{5.14}$$

and the initial conditions

$$w(\zeta, 0) = w_0 = \zeta^2. \tag{5.15}$$

Case 1: q-HASTA solution

To solve the Eqs (5.14) and (5.15) by using the Shehu transform with the initial condition, as

$$S[w(\zeta, \tau)] - \frac{u}{s}\zeta^2 + \frac{u^{\eta}}{s^{\eta}} S\left[\zeta \frac{\partial v}{\partial \zeta}\right] = 0. \tag{5.16}$$

The nonlinear operator defined by

$$\mathrm{N}[\chi(\zeta, \tau; \rho)] = S[\chi(\zeta, \tau; \rho)] - \frac{u}{s}\zeta^2 + \frac{u^{\eta}}{s^{\eta}} S\left[\zeta \frac{\partial \chi(\zeta, \tau; \rho)}{\partial \zeta}\right], \tag{5.17}$$

and thus

$$\Re(\vec{w}_{m-1}) = S(w_{m-1}) - \left(1 - \frac{k_m}{n}\right) \frac{u}{s}\zeta^2 + \frac{u^{\eta}}{s^{\eta}}\left[\zeta \frac{\partial w_{m-1}}{\partial \zeta}\right]. \tag{5.18}$$

The mth-order deformed equation is given as

$$S[w_m(\zeta, \tau) - k_m w_{m-1}(\zeta, \tau)] = \hbar \Re_m(\vec{w}_{m-1}). \tag{5.19}$$

Computing the inverse Shehu transform, we get

$$w_m(\zeta,\tau) = k_m w_{m-1}(\zeta,\tau) + \hbar L^{-1}\left[\Re_m(\vec{w}_{m-1})\right]. \tag{5.20}$$

Simplifying the Eq (5.20), for $m = 1, 2, 3, \cdots$, we get

$$v_1(\zeta,\tau) = 2\,\hbar\zeta^2 \frac{\tau^\eta}{\Gamma(\mu+1)},$$

$$v_2(\zeta,\tau) = 2\hbar\,(\hbar+n)\;\zeta^2\frac{\tau^\eta}{\Gamma(\eta+1)} + 4\hbar^2\,\zeta^2\frac{\tau^{2\eta}}{\Gamma(2\eta+1)},$$

$$v_3(\zeta,\tau) = 2\hbar\,(\hbar+n)^2\,\zeta^2\tfrac{\tau^\eta}{\Gamma(\eta+1)}e^\zeta + 8\hbar^2\,(\hbar+n)\;\zeta^2\tfrac{\tau^{2\eta}}{\Gamma(2\eta+1)} + 8\hbar^3\,\zeta^2\tfrac{\tau^{3\eta}}{\Gamma(3\eta+1)}, \tag{5.21}$$
$$\vdots$$

And so on, the components of $w_m(\zeta,\tau), m \geq 4$, can be easily obtained. Therefore, the approximate solution series given as

$$w(\zeta,\tau) = w_0(\zeta,\tau) + \sum_{m=1}^{\infty} w_m(\zeta,\tau)\left(\frac{1}{n}\right)^m. \tag{5.22}$$

If we select $\hbar = -1$, $n = 1$ and $\eta = 1$ then clearly, we can observe that the solution series (5.22), provide solution which is converges to the exact solution $w(\zeta,\tau) = \zeta^2 e^{-2\tau}$.

Case 2: RDTA solution

We apply the RDTA to Eq (5.14), we obtained the following relation

$$\frac{\Gamma(m\eta+\eta+1)}{\Gamma(m\eta+1)}W_{m+1} = -\zeta\frac{\partial W_m}{\partial\zeta}. \tag{5.23}$$

Using the RDTA with initial condition (5.15), we get

$$W_0(\zeta) = \zeta^2. \tag{5.24}$$

Solve the relation (5.23) and using Eq (5.24), we deduce the following components of $W_m(\zeta)$, for $m = 0, 1, 2, 3, \cdots$, as

$$W_1(\zeta) = -2\zeta^2\frac{1}{\Gamma(\eta+1)},\, W_2(\zeta) = 4\zeta^2\frac{1}{\Gamma(2\eta+1)},\, W_3(\zeta) = -8\zeta^2\frac{1}{\Gamma(3\eta+1)},$$

$$W_4(\zeta) = 16\zeta^2\frac{1}{\Gamma(4\eta+1)}, \tag{5.25}$$

and so on, the components of $w_m(\zeta,t)$ for $m > 4$ can be obtained and the RDTA approximate series solution deduced as

$$w(\zeta,\tau) = \sum_{m=0}^{\infty} W_m(\zeta)\,\tau^{m\eta}. = W_0(\zeta) + W_1(\zeta)\,\tau^\eta + W_2(\zeta)\tau^{2\eta} + W_3(\zeta)\,\tau^{3\eta} + W_4(\zeta)\,\tau^{4\eta} + \cdots$$

$$= \zeta^2 - 2\zeta^2\frac{\tau^\eta}{\Gamma(\eta+1)} + 4\zeta^2\frac{\tau^{2\eta}}{\Gamma(2\eta+1)} - 8\zeta^2\frac{\tau^{3\eta}}{\Gamma(3\eta+1)} + 16\zeta^2\frac{\tau^{4\eta}}{\Gamma(4\eta+1)} + \cdots. \tag{5.26}$$

When we select $\eta = 1$ then the series (5.26), rapidly converges to the exact solution

$$w(\zeta, \tau) = \zeta^2 e^{-2\tau}. \tag{5.27}$$

The above result (5.26) is in complete agreement with the q-HASTA ($\hbar = -1, n = 1$) and VIM [15] at $\eta = 1$.

The numerical analysis for the approximate solution of Eq (5.14) obtained by using the q-HASTA & the RDTA and the original solution (5.13) in Figures 6–10 are computed by using maple package.

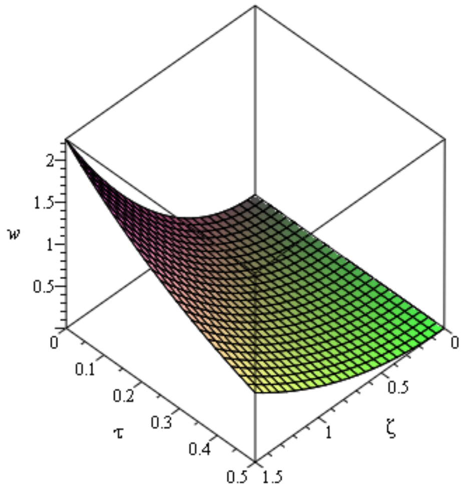

Figure 6. The surface shows the exact solution $w(\zeta, \tau)$ v/s space variable ζ and time variable τ.

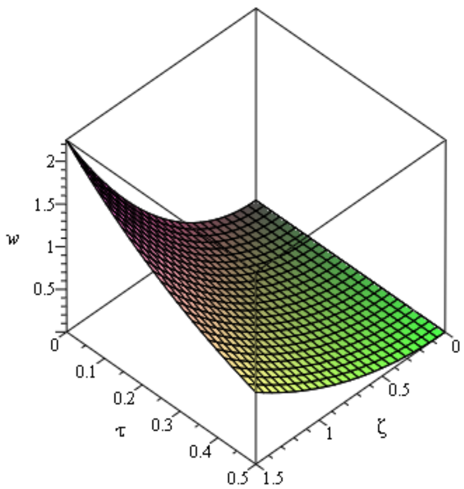

Figure 7. The surface shows the RDTA (q-HASTA, $\hbar = -1$, $n = 1$) solution $w(\zeta, \tau)$ v/s space variable ζ and time variable τ at $\eta = 1$.

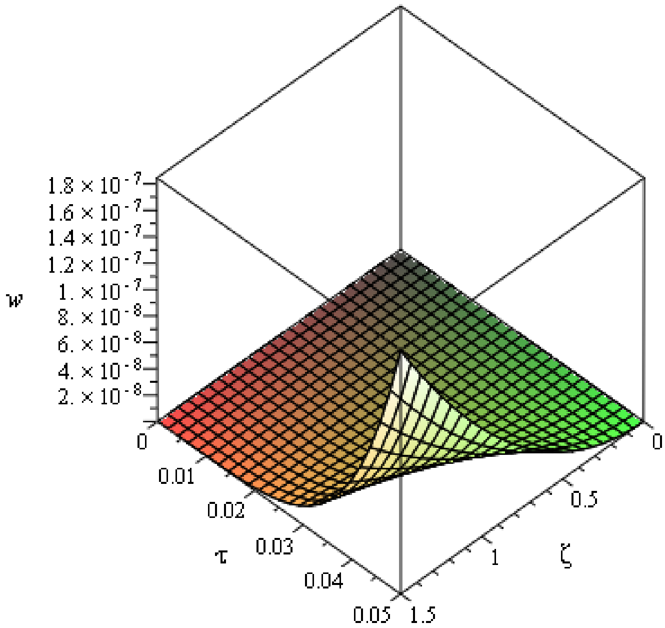

Figure 8. The surface represented the absolute error $E_4(w) = \left|w_{ex.} - w_{apr.}\right|$ v/s space variable ζ and time variable τ at $\hbar = -1, n = 1, \eta = 1$.

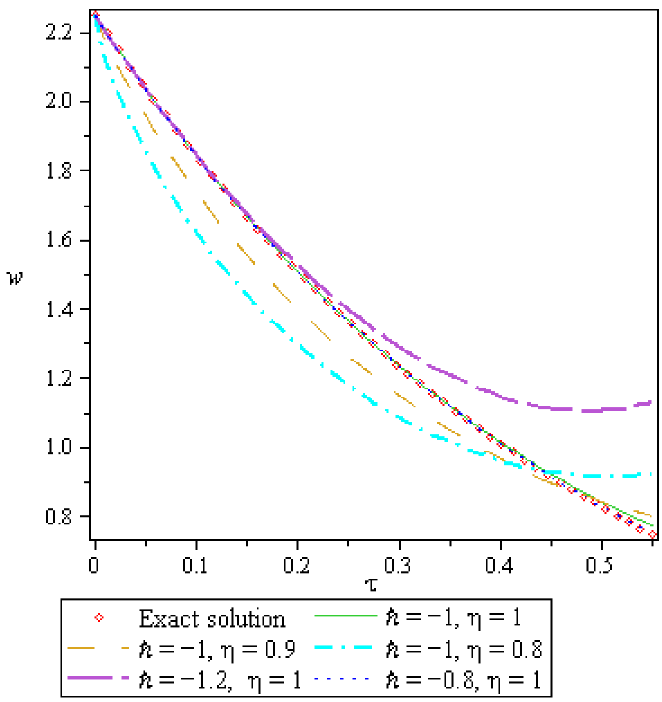

Figure 9. Comprehensive study b/w exact solution, RDTA solution ($\hbar = -1$) and the family of q-HASTA solutions v/s time variable τ at space variable $\zeta = 1.5$ and $n = 1$.

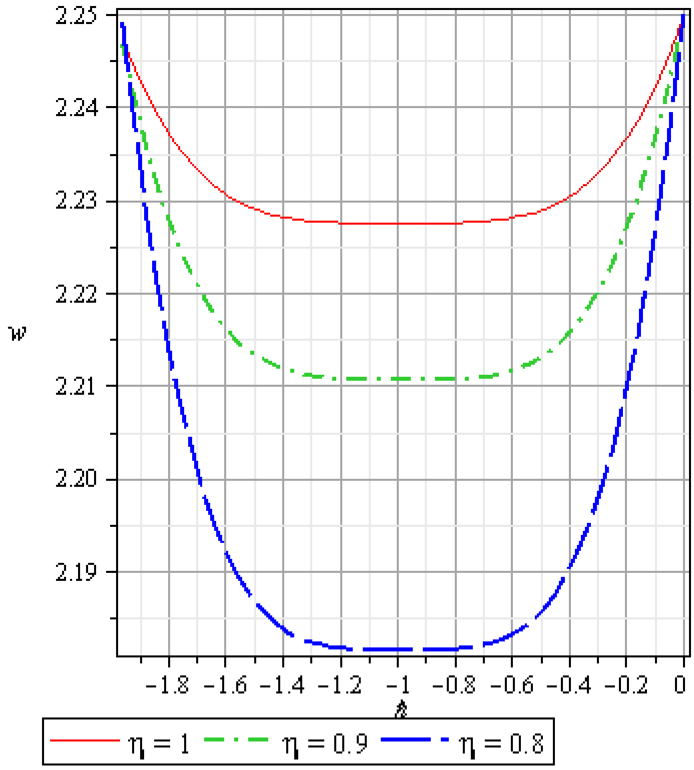

Figure 10. $\hbar$ − *curves* for comparative study of q-HASTA for varies values of η at $\zeta = 1.5$, $\tau = 0.005$ and $n = 1$.

Example 3. Next, we take the fractional non-homogeneous equation

$$\frac{\partial^{\eta} w}{\partial \tau^{\eta}} + \frac{\partial w}{\partial \zeta} = \zeta, \tag{5.28}$$

and the initial conditions

$$w(\zeta, 0) = w_0 = e^{\zeta}. \tag{5.29}$$

Case 1: q-HASTA solution

Taking the Shehu transform of Eq (5.28) and using condition (5.29), as

$$S\left[w(\zeta, \tau)\right] - \frac{u}{s} e^{\zeta} + \frac{u^{\eta}}{s^{\eta}} S\left[\frac{\partial w}{\partial \zeta} - \zeta\right] = 0. \tag{5.30}$$

The nonlinear operator is

$$\mathrm{N}\left[\chi(\zeta, \tau; \rho)\right] = S\left[\chi(\zeta, \tau; \rho)\right] - \frac{u}{s} e^{\zeta} + \frac{u^{\eta}}{s^{\eta}} S\left[\frac{\partial \chi(\zeta, \tau; \rho)}{\partial \zeta} - \zeta\right], \tag{5.31}$$

and we have

$$\Re(\vec{w}_{m-1}) = S(w_{m-1}) - (1 - \frac{k_m}{n}) \frac{u}{s} e^{\zeta} + \frac{u^{\eta}}{s^{\eta}} S\left[\frac{\partial w}{\partial \zeta} - (1 - \frac{k_m}{n}) \zeta\right]. \tag{5.32}$$

The mth-order deformed equation is defined as

$$S\left[w_m(\zeta,\tau)-k_m w_{m-1}(\zeta,\tau)\right]=\hbar\Re_m(\vec{w}_{m-1}). \tag{5.33}$$

The inverse Shehu transform of (5.33), we have

$$w_m(\zeta,\tau)=k_m w_{m-1}(\zeta,\tau)+\hbar S^{-1}\left[\Re_m(\vec{w}_{m-1})\right]. \tag{5.34}$$

For $m=1,2,3,\cdots$, simplifying the Eq (5.34), we deduce

$$\begin{aligned}
w_1(\zeta,\tau)&=\hbar(e^{\zeta}-\zeta)\frac{\tau^{\eta}}{\Gamma(\eta+1)},\\
w_2(\zeta,\tau)&=\hbar\,(\hbar+n)\,(e^{\zeta}-\zeta)\frac{\tau^{\eta}}{\Gamma\,(\eta+1)}+\hbar^2(e^{\zeta}-1)\frac{\tau^{2\eta}}{\Gamma\,(2\eta+1)},\\
w_3(\zeta,\tau)&=\hbar\,(\hbar+n)^2\,(e^{\zeta}-\zeta)\frac{\tau^{\eta}}{\Gamma\,(\eta+1)}+2\hbar^2(e^{\zeta}-1)\frac{\tau^{2\eta}}{\Gamma\,(2\eta+1)}+\hbar^3e^{\zeta}\frac{\tau^{3\eta}}{\Gamma\,(3\eta+1)},\\
&\vdots
\end{aligned} \tag{5.35}$$

and so on, the components of $w_m(\zeta,\tau), m>3$, can be easily computed and the series solution is given by

$$w(\zeta,\tau)=w_0(\zeta,\tau)+\sum_{m=1}^{\infty}w_m(\zeta,\tau)\left(\frac{1}{n}\right)^m. \tag{5.36}$$

If we select $\hbar=-1$, $n=1$ and $\eta=1$ then clearly, the series solution (5.36) converges to the exact solution $w(\zeta,\tau)=\tau(\zeta-\frac{t}{2})+e^{\zeta-\tau}$.

Case 2: RDTA solution

We use the RDTA to Eq (5.28), we obtained the following relation

$$\frac{\Gamma(m\eta+\eta+1)}{\Gamma(m\eta+1)}W_{m+1}=\zeta(1-k_m)-\frac{\partial W_m}{\partial\zeta}, \tag{5.37}$$

the RDTA to the initial condition (5.37), we have

$$W_0(\zeta)=\zeta^2. \tag{5.38}$$

Apply Eq (5.38) in Eq (5.37), we get the following components of $W_m(\zeta)$, for $m=0,1,2,3,\cdots$,

$$\begin{gathered}
W_1(\zeta)=-\left(e^{\zeta}-\zeta\right)\frac{1}{\Gamma(\eta+1)},\, W_2(\zeta)=\left(e^{\zeta}-1\right)\frac{1}{\Gamma\,(2\eta+1)},\, W_3(\zeta)=-e^{\zeta}\frac{1}{\Gamma\,(3\eta+1)},\\
W_4(\zeta)=e^{\zeta}\tfrac{1}{\Gamma(4\eta+1)},\\
\vdots
\end{gathered} \tag{5.39}$$

And so on, the components of $w_m(\zeta,\tau)$ can be easily obtained and the RDTA approximate series solution deduced as

$$w(\zeta,\tau) = \sum_{m=0}^{\infty} W_m(\zeta)\,\tau^{m\eta}. = W_0(\zeta) + W_1(\zeta)\,\tau^{\eta} + W_2(\zeta)\,\tau^{2\eta} + W_3(\zeta)\,\tau^{3\eta} + W_4(\zeta)\,\tau^{4\eta} + \cdots$$

$$= \zeta^2 - (e^{\zeta} - \zeta)\frac{\tau^{\eta}}{\Gamma(\eta+1)} + (e^{\zeta} - 1)\frac{\tau^{2\eta}}{\Gamma(2\eta+1)} - e^{\zeta}\frac{\tau^{3\eta}}{\Gamma(3\eta+1)} + e^{\zeta}\frac{\tau^{4\eta}}{\Gamma(4\eta+1)} - \cdots. \quad (5.40)$$

Which is the same as deduced by the q-HASTA ($\hbar = -1, n = 1$) and VIM [15] at $\eta = 1$. We observed that the solution series (5.40) at $\eta = 1$, converges to the exact solution

$$w(\zeta,\tau) = \tau(\zeta - \frac{\tau}{2}) + e^{\zeta-\tau}. \quad (5.41)$$

The numerical simulations of the approximate solution (5.28) deduced by using the q-HASTA & the RDTA and the exact solution (5.41) are depicted in Figures 11–16.

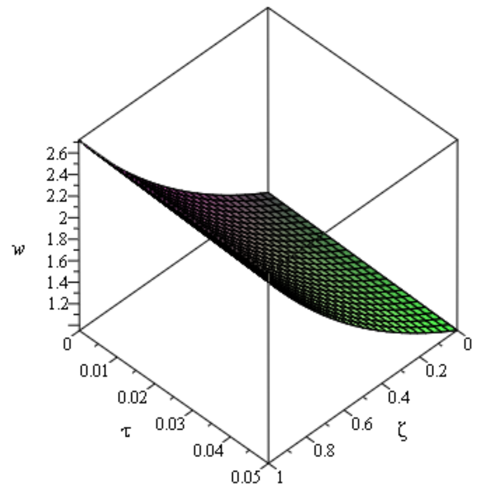

Figure 11. The surface shows the exact solution $w(\zeta,\tau)$ v/s space variable ζ and time variable τ.

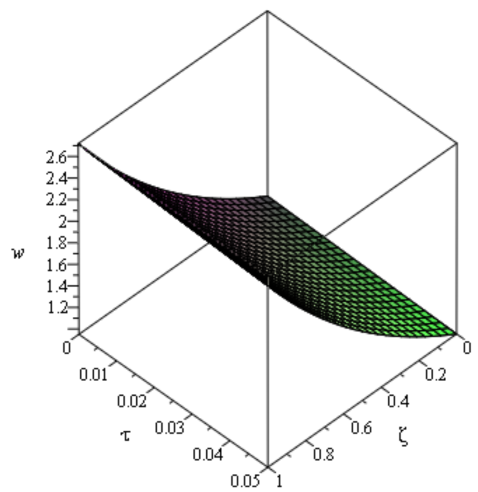

Figure 12. The surface shows the RDTA (q-HASTA, $\hbar = -1,\ n = 1$) solution $w(\zeta,\tau)$ v/s space variable ζ and time variable τ at $\eta = 1$.

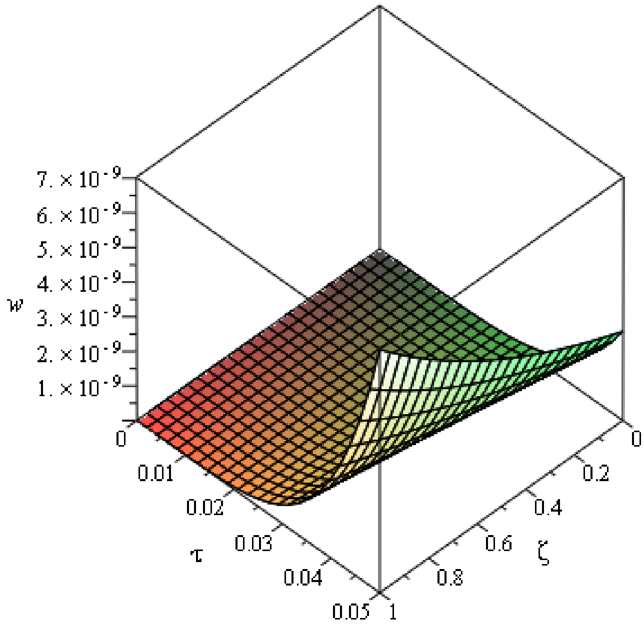

Figure 13. The surface shows the absolute error $E_4(w) = \left|w_{ex.} - w_{apr.}\right|$ v/s space variable ζ and time variable τ at $\hbar = -1, n = 1,\ \eta = 1$.

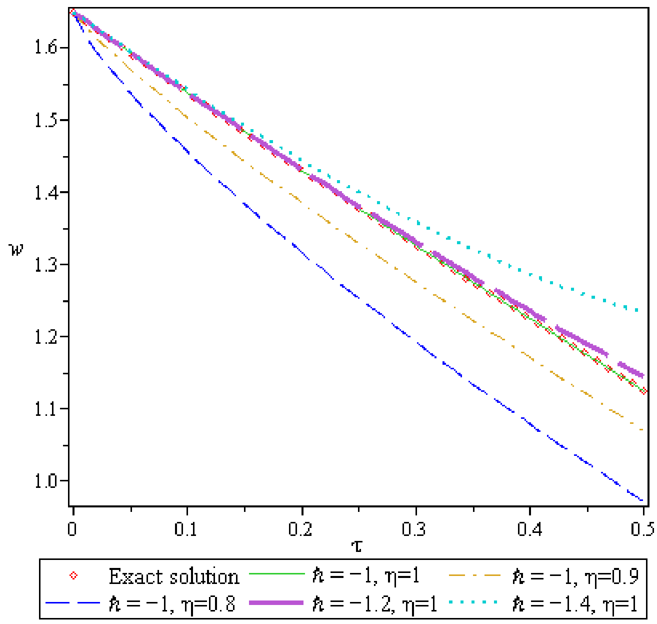

Figure 14. Comprehensive study b/w exact solution, RDTA solution ($\hbar = -1$) and the family of q-HASTA solutions v/s time variable τ at space variable $\zeta = 1.5$ and $n = 1$.

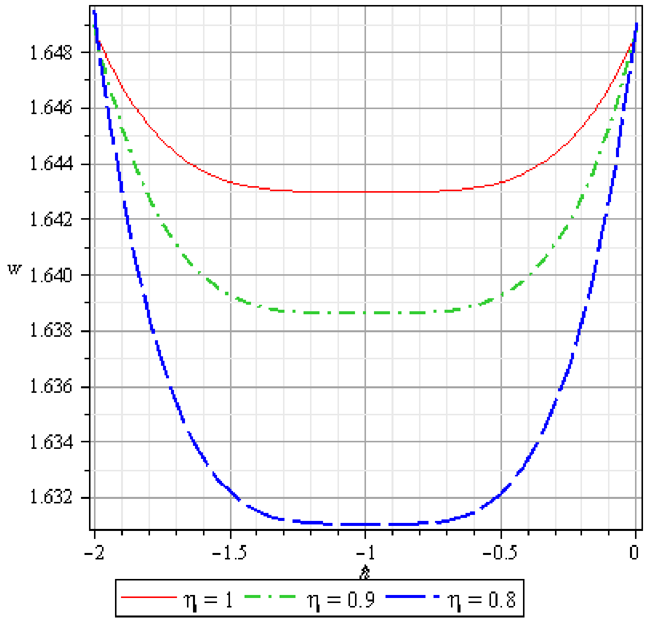

Figure 15. $\hbar-$ *curves* comparative study of q-HASTA for varies η at $\zeta = 0.5,\ \tau = 0.005$ and $n = 1$.

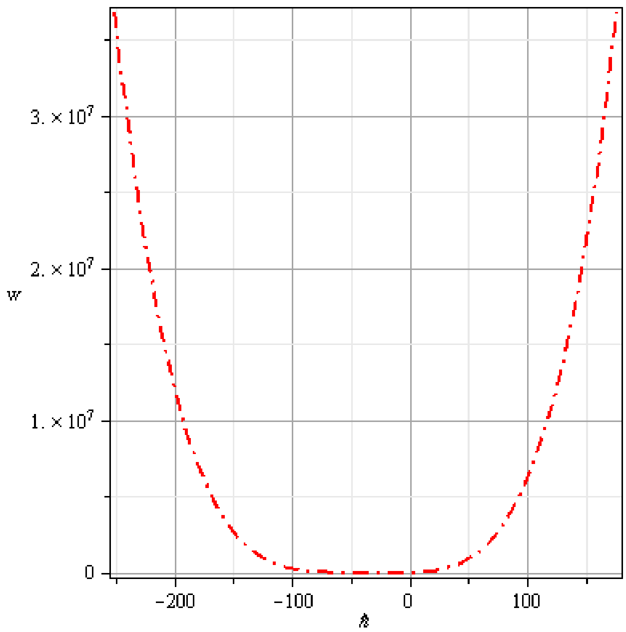

Figure 16. $\hbar-$ *curve* for q-HASTA solution at $\zeta = 0.5,\ \tau = 0.005, n = 50$ and $\eta = 1$.

Example 4. Now, we consider the inviscid Bugers' equation in fractional form as

$$\frac{\partial^{\eta} w}{\partial \tau^{\eta}} + w\frac{\partial w}{\partial \zeta} = 0, \tag{5.42}$$

and the initial conditions

$$w(\zeta,0)=w_0=\zeta,\quad \zeta\in R. \tag{5.43}$$

Case 1: q-HASTA solution

Taking the Shehu transform of Eq (5.42) with the initial condition (5.43), we have

$$S\left[w(\zeta,\tau)\right]-\frac{u}{s}\zeta+\frac{u^{\eta}}{s^{\eta}}S\left[w\frac{\partial w}{\partial\zeta}\right]=0. \tag{5.44}$$

The nonlinear operator is

$$\mathrm{N}\left[\chi(\zeta,\tau;\rho)\right]=S\left[\chi(\zeta,\tau;\rho)\right]-\frac{u}{s}\zeta+\frac{u^{\eta}}{s^{\eta}}S\left[\chi(\zeta,\tau;\rho)\frac{\partial\chi(\zeta,\tau;\rho)}{\partial\zeta}\right], \tag{5.45}$$

and thus

$$\Re_m(\vec{w}_{m-1})=S(w_{m-1})-(1-\frac{k_m}{n})\frac{u}{s}\zeta+\frac{u^{\eta}}{s^{\eta}}L\left[\sum_{i=0}^{m-1}w_i\frac{\partial w_{m-i-1}}{\partial\zeta}\right]. \tag{5.46}$$

The mth-order deformed equation is given as

$$S\left[w_m(\zeta,\tau)-k_m w_{m-1}(\zeta,\tau)\right]=\hbar\Re_m(\vec{w}_{m-1}). \tag{5.47}$$

The inverse Shehu transform of (5.47), we get

$$w_m(\zeta,\tau)=k_m w_{m-1}(\zeta,\tau)+\hbar S^{-1}\left[\Re_m(\vec{w}_{m-1})\right]. \tag{5.48}$$

For $m=1,2,3,\cdots$, simplifying the above Eq (5.48), we get

$$\begin{aligned}
w_1(\zeta,\tau)&=\hbar\zeta\frac{\tau^{\eta}}{\Gamma(\eta+1)},\\
w_2(\zeta,\tau)&=\hbar(\hbar+n)\zeta\frac{\tau^{\eta}}{\Gamma(\eta+1)}+2\hbar^2\zeta\frac{\tau^{2\eta}}{\Gamma(2\eta+1)},\\
w_3(\zeta,\tau)&=\hbar(\hbar+n)^2\zeta\tfrac{\tau^{\eta}}{\Gamma(\eta+1)}+2\hbar(\hbar+n)^2\zeta\tfrac{\tau^{2\eta}}{\Gamma(2\eta+1)}+4\hbar^3\zeta\tfrac{\tau^{3\eta}}{\Gamma(3\eta+1)}\\
&\quad+\hbar^3\zeta\tfrac{\tau^{3\eta}}{\Gamma(3\eta+1)}\tfrac{\Gamma(2\eta+1)}{(\Gamma(\eta+1))^2},\\
&\ \ \vdots
\end{aligned} \tag{5.49}$$

Iterating in this procedure, the components of $w_m(\zeta,\tau), m>3$, can be easily computed and the series solutions are determined by

$$w(\zeta,\tau)=w_0(\zeta,\tau)+\sum_{m=1}^{\infty}w_m(\zeta,\tau)(1/n)^m. \tag{5.50}$$

If we select $\hbar-1, n=1$ and $\eta=1$, then the solution series (5.53) convert to $w(\zeta,\tau)=\zeta-\tau\zeta+\tau^2\zeta-\tau^3\zeta+\tau^4\zeta-\cdots+(-1)^r\tau^r\zeta+\cdots=\zeta(1+\tau)^{-1}$, which is exactly same as obtained by VIM [15].

Case 2: RDTA solution

Now we apply the RDTA to Eq (5.42), we get the following recurrence relation

$$\frac{\Gamma(m\eta+\eta+1)}{\Gamma(m\eta+1)}W_{m+1} = -\sum_{i=0}^{m} W_i \frac{\partial W_{m-i}}{\partial \zeta}, \tag{5.51}$$

apply the RDTA with the initial condition (5.43), we get

$$W_0(\zeta) = \zeta. \tag{5.52}$$

Apply Eq (5.52) in Eq (5.51), we get the components of $W_m(\zeta)$, for $m = 0, 1, 2, 3, \cdots$, as

$$W_1(\zeta) = -\zeta\frac{1}{\Gamma(\eta+1)}, W_2(\zeta) = 2\zeta\frac{1}{\Gamma(2\eta+1)}, W_3(\zeta) = -\zeta\frac{\Gamma(2\eta+1)}{\Gamma(3\eta+1)\Gamma(\eta+1)^2} - 4\zeta\frac{1}{\Gamma(3\eta+1)},$$

$$W_4(\zeta) = 2\zeta\frac{\Gamma(2\eta+1)}{\Gamma(4\eta+1)\Gamma(\eta+1)^2} + 4\zeta\frac{\Gamma(3\eta+1)}{\Gamma(\eta+1)\Gamma(2\eta+1)\Gamma(4\eta+1)} + 8\zeta\frac{1}{\Gamma(4\eta+1)},$$
$$\vdots \tag{5.53}$$

In this processes, the components of $w_m(\zeta, \tau), m > 4$, can be easily found and the RDTA approximate solution deduced as

$$w(\zeta,\tau) = \sum_{m=0}^{\infty} W_m(\zeta)\,\tau^{m\eta} = W_0(\zeta) + W_1(\zeta)\,\tau^{\eta} + W_2(\zeta)\tau^{2\eta} + W_3(\zeta)\,\tau^{3\eta} + W_4(\zeta)\,\tau^{4\eta} + \cdots$$

$$= \zeta - \zeta\frac{\tau^{\eta}}{\Gamma(\eta+1)} + 2\zeta\frac{\tau^{2\eta}}{\Gamma(2\eta+1)} - \zeta\frac{\Gamma(2\eta+1)\,\tau^{3\eta}}{\Gamma(3\eta+1)\Gamma(\eta+1)^2} - 4\zeta\frac{\tau^{3\eta}}{\Gamma(3\eta+1)}$$

$$+2\zeta\frac{\Gamma(2\eta+1)\,\tau^{4\eta}}{\Gamma(4\eta+1)\Gamma(\eta+1)^2} + 4\zeta\frac{\Gamma(3\eta+1)\,\tau^{4\eta}}{\Gamma(\eta+1)\Gamma(2\eta+1)\Gamma(4\eta+1)} + 8\zeta\frac{\tau^{4\eta}}{\Gamma(4\eta+1)} - \cdots. \tag{5.54}$$

Which is the coincident with the solution series deduced by q-HASTA ($\hbar = -1, n = 1$) and obtained by VIM [15] at $\eta = 1$. The solution series (5.54), $\sum_{m=0}^{\infty} W_m(\zeta)\,\tau^{m\eta}$ convert to exact solution at $\eta = 1$, given as

$$w(\zeta,\tau) = \zeta(1+\tau)^{-1}. \tag{5.55}$$

The numerical results of (5.42) deduced from the q-HASTA and the RDTA, and the exact solution (5.55) are depicted in Figures 17–22 and in Table 3.

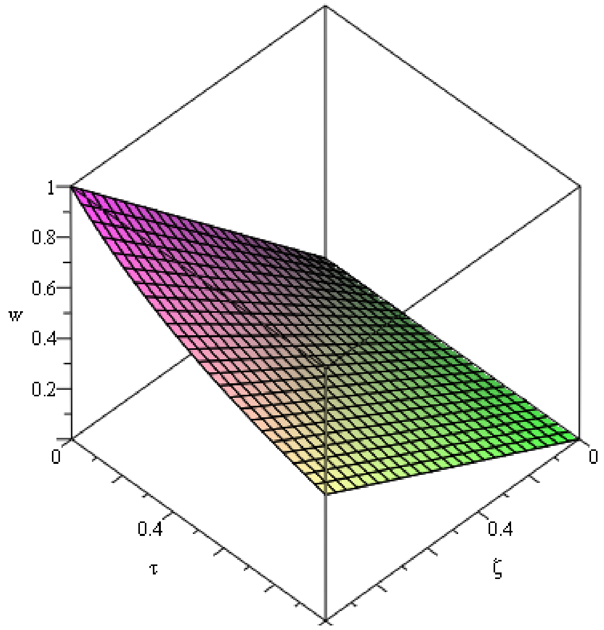

Figure 17. The surface shows the exact solution $w(\zeta, \tau)$ v/s space variable ζ and time variable τ.

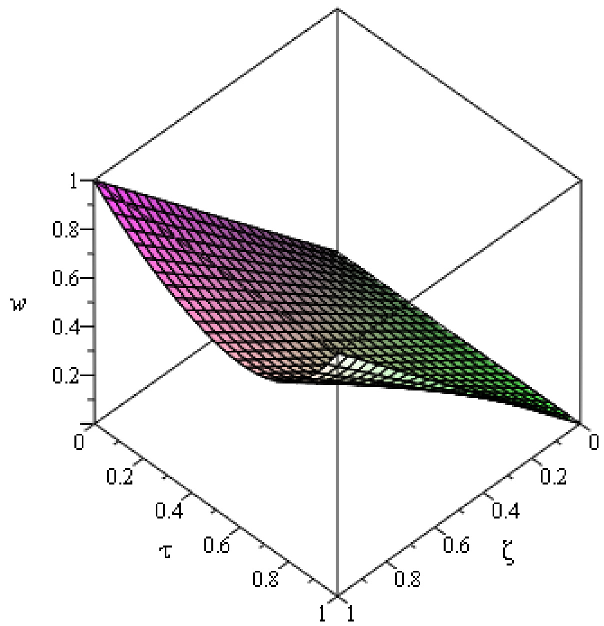

Figure 18. The nature of RDTA (q-HASTA, $\hbar = -1$, $n = 1$) solution $w(\zeta, \tau)$ v/s space variable ζ and time variable τ at $\eta = 1$.

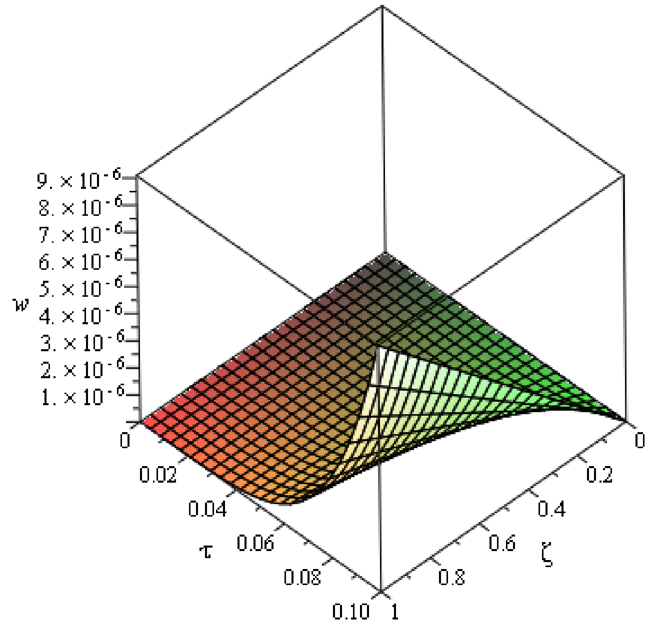

Figure 19. The surface shows the absolute error $E_4(w) = \left|w_{ex.} - w_{apr.}\right|$ v/s space variable ζ and time variable τ at $\hbar = -1, n = 1,\ \eta = 1$.

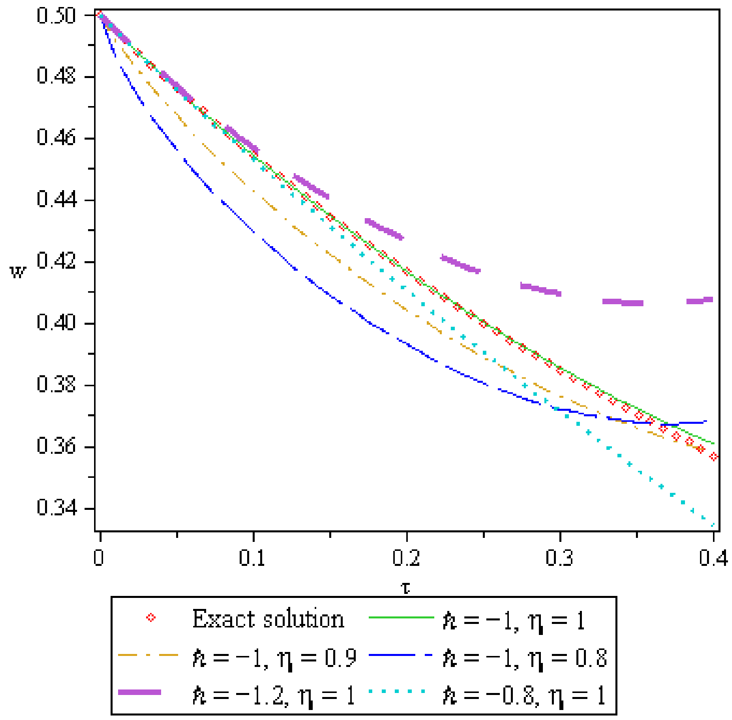

Figure 20. Comprehensive nature b/w exact solution, RDTA solution ($\hbar = -1$) and the family of q-HASTA solutions v/s time variable τ at space variable $\zeta = 1.5$ and $n = 1$.

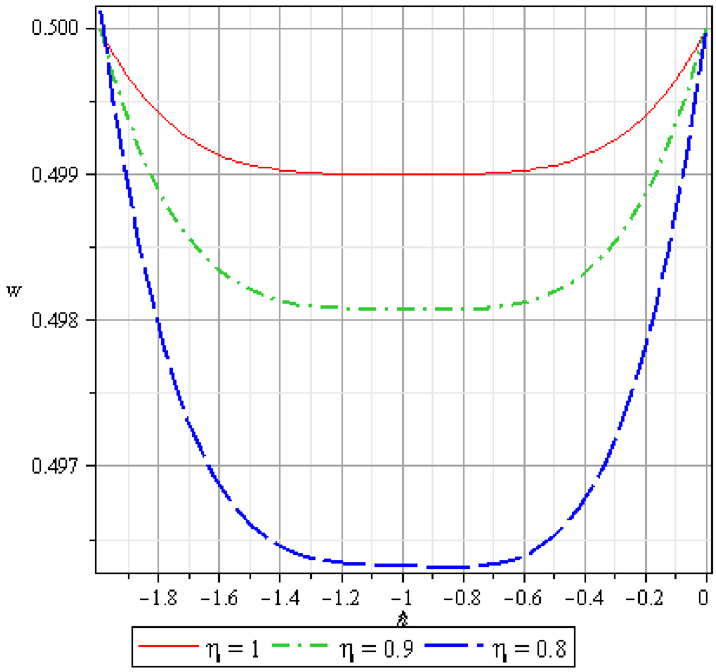

Figure 21. $\hbar$ − *curves* comparative behave of q-HASTA for varies η at $\varsigma = 0.5$, $\tau = 0.002$ and $n = 1$.

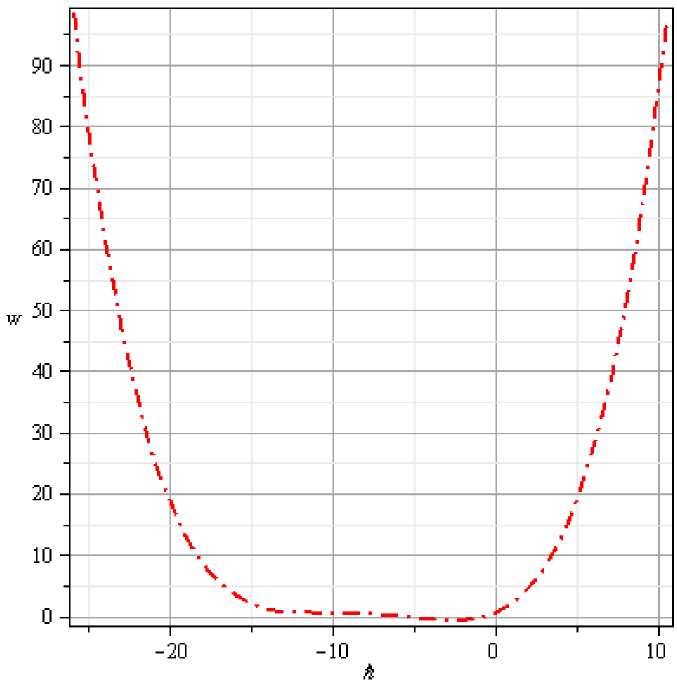

Figure 22. $\hbar$ − *curve* for q-HASTA solution at $\zeta = 0.5$, $\tau = 0.002, n = 10$ and $\eta = 1$.

Table 3. Comparative study for q-HASTA at $\zeta = 0.5, \eta = 1$.

τ	Exact solution	q-HASTA ($\hbar = -1, n = 1$)		q-HASTA $\hbar = -1, n = 2$	
		Approximate solution	Absolute error	Approximate solution	Absolute error
0	0.5	0.5	0	0.5	0
0.01	0.4950495050	0.4950495000	0.5000000×10^{-9}	0.4849995000	1.0050005×10^{-2}
0.02	0.4901960784	0.4901960000	7.8400000×10^{-8}	0.4699960000	2.0200078×10^{-2}
0.03	0.4854368932	0.4854365000	3.9320000×10^{-7}	0.4549865000	3.0450393×10^{-2}
0.04	0.4807692308	0.4807680000	1.2308000×10^{-6}	0.4399680000	4.0801230×10^{-2}
0.05	0.4761904762	0.4761875000	2.9762000×10^{-6}	0.4249375000	5.1252976×10^{-2}

6. Results and discussion

We observed from the numerical results and from graphically representations (Figures 1–22) of the fractional Cauchy problems v/s space variable $\zeta$and time variable τ with order of fractional derivatives. The q-HASTA control the convergence of the solution series by using the appropriate values of auxiliary parameters $\hbar$ and n at large admissible domain. $\hbar - curves$ show that the validated convergence range and also the horizontal line segments denoted the range for convergence of solution series. We observe that the convergence region directly proportional to auxiliary parameter n have the advantage of the q-HASTA to the HAM, which is depicted in Figures 16 and 22. We also observed that the HAM (q-HASTA, $n = 1$) and RDTA, VIM (q-HASTA, $\hbar = -n$) are special cases of q-HASTA. Maple plotting represents the comparative approximate solutions behavior of the RDTA and the q-HASTA v/s exact and existing solutions.

7. Conclusions

In this paper, we successfully applied computational algorithm namely q-HASTA and compared with the RDTA for solving the time fractional Cauchy equations and found the approximate solution series, closed to the exact solution. We observed that the RDTA is special condition of the q-HASTA. The q-HASTA is provide many more options for the interest of the convergence region by taking the number of parameters and auxiliary functions, whereas the RDTA algorithm provides solution series components from recursive relation, easy computational work, coming complex calculations and reducing the time and size of calculations.

Acknowledgments

The authors extend their appreciation to the Deputyship for research and innovation, Ministry of Education in Saudi Arabia for funding this research work through the project number IF-PSAU-2021/01/17698.

Conflict of interest

The authors declare that there are no conflicts of interest regarding the publication of this paper.

References

1. M. Caputo, Linear model of dissipation whose Q is almost frequency independent-II, *Geophys. J. Int.*, **13** (1967), 529–539. https://doi.org/10.1111/j.1365-246X.1967.tb02303.x
2. M. Caputo, *Elasticità e dissipazione*, Zani-Chelli, Bologna 1969.
3. K. B. Oldham, J. Spanier, *The fractional calculus: Theory and application of differentiation and integration to arbitrary order*, New York: Academic Press, 1974.
4. M. Hedayati, R. Ezzati, S. Noeiaghdam, New procedures of a fractional order model of novel coronavirus (COVID-19) outbreak via wavelets method, *Axioms*, **10** (2021), 1–23. https://doi.org/10.3390/axioms10020122
5. A. Carpinteri, F. Mainardi, *Fractional calculus in continuum mechanics*, New York: Springer, 1997.
6. I. Podlubny, *Fractional differential equations*, San Diego, Calif: Academic Press, 1999.
7. A. A. Kilbas, H. M. Srivastava, J. J. Trujillo, *Theory and applications of fractional differential equations*, Amsterdam: Elsevier, 2006.
8. H. Bulut, H. M. Baskonus, Y. Pandir, The modified trial equation method for fractional wave equation and time-fractional generalized Burgers equation, *Abstr. Appl. Anal.*, **2013** (2013), 1–8. https://doi.org/10.1155/2013/636802
9. J. H. He, Approximate analytical solution for seepage flow with fractional derivatives in porous media, *Comput. Methods Appl. Mech. Eng.*, **167** (1998), 57–58. https://doi.org/10.1016/S0045-7825(98)00108-X
10. V. P. Dubey, R. Kumar, D. Kumar, A hybrid analytical scheme for the numerical computation of time fractional computer virus propagation model and its stability analysis, *Chaos Soliton. Fract.*, **133** (2020), 109626. https://doi.org/10.1016/j.chaos.2020.109626
11. S. Kumar, Y. Khan, A. Yildirim, A mathematical modelling arising in the chemical system and its approximate numerical solution, *Asia Pacific J. Chem. Eng.*, **7** (2012), 835–840. https://doi.org/10.1002/apj.647
12. J. Singh, D. Kumar, S. D. Purohit, A. M. Mishra, M. Bohra, An efficient numerical approach for fractional multi-dimensional diffusion equations with exponential memory, *Numer. Methods Partial Differ. Eq.*, **37** (2021), 1631–1651. https://doi.org/10.1002/num.22601
13. Ramswroop, J. Singh, D. Kumar, Numerical computation of fractional Lotka-Volterra equation arising in biological systems, *Nonlinear Eng.*, **4** (2015), 117–125. https://doi.org/10.1515/nleng-2015-0012
14. B. Ghanbari, D. Kumar, Numerical solution of predator-prey model with Beddington-DeAngelis functional response and fractional derivatives with Mittag-Leffler kernel, *Chaos*, **29** (2019), 063103. https://doi.org/10.1063/1.5094546

15. X. W. Zhou, L. Yao, The variation iteration method for Cauchy problems, *Comput. Math. Appl.*, **60** (2010), 756–760. https://doi.org/10.1016/j.camwa.2010.05.022
16. R. C. McOwn, *Partial differential equation: Method and applications*, Prentice Hall, Inc., 1996.
17. A. Tveito, R. Winther, *Interoduction to partial differential equations*, Berlin, Heidelberg: Springer-Verlag, 2005.
18. N. H. Asmar, *Partial differential equations with Fourier series and boundary value problems*, Prentice Hall, Inc., 2004.
19. V. P. Dubey, R. Kumar, D. Kumar, A reliable treatment of residual power series method for time-fractional Black-Scholes European option pricing equations, *Phys. A*, **533** (2019), 122040. https://doi.org/10.1016/j.physa.2019.122040
20. S. Maitama, W. Zhao, New Laplace-type integral transform for solving steady heat transfer problem, *Therm. Sci.*, **25** (2021), 1–12. https://doi.org/10.2298/TSCI180110160M
21. S. Maitama, W. Zhao, New integral transform: Shehu transform a generalization of Sumudu and Laplace transform for solving differential equations, *Int. J. Anal. Appl.*, **17** (2019), 167–190. https://doi.org/10.28924/2291-8639-17-2019-167
22. R. Belgacem, D. Baleanu, A. Bokhari, Shehu transform and application to Caputo-fractional differential equations, *Int. J. Anal. Appl.*, **17** (2019), 917–927.
23. A. Bokhari, D. Baleanu, R. Belgacem, Application of Shehu transform to Atangana-Baleanu derivatives, *J. Math. Comput. Sci.*, **20** (2019), 101–107. http://dx.doi.org/10.22436/jmcs.020.02.03
24. M. A. El-Tawil, S. Huseen, The q-homotopy analysis method (q-HAM), *Int. J. Appl. Math. Mech.*, **8** (2012), 51–75.
25. M. A. El-Tawil, S. Huseen, On convergence of the q-homotopy analysis method, *Int. J. Conte. Math. Sci.*, **8** (2013), 481–497.
26. S. J. Liao, *The proposed homotopy analysis technique for the solution of nonlinear problems*, Ph.D. Thesis, Shanghai Jiao Tong University, 1992.
27. S. J. Liao, *Beyond perturbation: Introduction to the homotopy analysis method*, Boca Raton: Chaoman and Hall/CRC Press, 2003.
28. S. J. Liao, On the homotopy analysis method for nonlinear problems, *Appl. Math. Comput.*, **147** (2004), 499–513. https://doi.org/10.1016/S0096-3003(02)00790-7
29. S. J. Liao, K. F. Cheung, Homotopy analysis of nonlinear progressive waves in deep water, *J. Eng. Math.*, **45** (2003), 105–116. https://doi.org/10.1023/A:1022189509293
30. S. Noeiaghdam, M. Suleman, H. Budak, Solving a modified nonlinear epidemiological model of computer viruses by homotopy analysis method, *Math. Sci.*, **12** (2018), 211–222. https://doi.org/10.1007/s40096-018-0261-5
31. S. Noeiaghdam, S. Micula, Dynamical strategy to control the accuracy of the nonlinear bio-mathematical model of malaria infection, *Mathematics*, **9** (2021), 1031. https://doi.org/10.3390/math9091031
32. S. Noeiaghdam, S. Micula, J. J. Nieto, A novel technique to control the accuracy of a nonlinear fractional order model of COVID-19: Application of the CESTAC method and the CADNA library, *Mathematics*, **9** (2021), 1321. https://doi.org/10.3390/math9121321

33. S. Noeiaghdam, E. Zarei, H. B. Kelishami, Homotopy analysis transform method for solving Abel's integral equations of the first kind, *Ain Shams Eng. J.*, **7** (2016), 483–495. https://doi.org/10.1016/j.asej.2015.03.006

34. J. Singh, D. Kumar, R. Swroop, S. Kumar, An efficient computational approach for time-fractional Rosenau-Hyman equation, *Neural Comput. Appl.*, **30** (2018), 3063–3070. https://doi.org/10.1007/s00521-017-2909-8

35. Y. Keskin, G. Oturanc, Reduced differential transform method: A new approach to factional partial differential equations, *Nonlinear Sci. Lett. A*, **1** (2010), 61–72.

36. P. K. Gupta, Approximate analytical solutions of fractional Benney-Lin equation by reduced differential transform method and the homotopy perturbation method, *Comput. Math. Appl.*, **58** (2011), 2829–2842. https://doi.org/10.1016/j.camwa.2011.03.057

37. V. K. Srivastava, M. K. Awasthi, M. Tamsir, RDTM solution of Caputo time fractional-order hyperbolic telegraph equation, *AIP Adv.*, **3** (2013), 032142. https://doi.org/10.1063/1.4799548

38. J. Singh, Analysis of fractional blood alcohol model with composite fractional derivative, *Chaos, Soliton. Fract.*, **140** (2020), 110127. https://doi.org/10.1016/j.chaos.2020.110127

39. J. Singh, B. Ganbari, D. Kumar, D. Baleanu, Analysis of fractional model of guava for biological pest control with memory effect, *J. Adv. Res.*, **32** (2021), 99–108. https://doi.org/10.1016/j.jare.2020.12.004

40. V. P. Dubey, J. Singh, A. M. Alshehri, S. Dube, D. Kumar, Analysis of local fractional coupled Helmholtz and coupled Burgers' equations in fractal media, *AIMS Math.*, **7** (2022), 8080–8111. https://doi.org/10.3934/math.2022450

41. V. P. Dubey, J. Singh, A. M. Alshehri, S. Dubey, D. Kumar, An efficient analytical scheme with convergence analysis for computational study of local fractional Schrödinger equations, *Math. Comput. Simul.*, **196** (2022), 296–318. https://doi.org/10.1016/j.matcom.2022.01.012

42. S. Yadav, D. Kumar, J. Singh, D. Baleanu, Analysis and dynamics of fractional order COVID-19 model with memory effect, *Results Phys.*, **24** (2021), 104017. https://doi.org/10.1016/j.rinp.2021.104017

43. Y. Luchko, R. Gorenflo, An operational method for solving fractional differential equations with the Caputo derivatives, *Acta Math. Vietnam.*, **24** (1999), 207–233.

AIMS Press